

Published in final edited form as:

Science. 2013 October 18; 342(6156): . doi:10.1126/science.1241224.

Sleep Drives Metabolite Clearance from the Adult Brain

Lulu Xie^{1,*}, Hongyi Kang^{1,*}, Qiwu Xu¹, Michael J. Chen¹, Yonghong Liao¹, Meenakshisundaram Thiyagarajan¹, John O'Donnell¹, Daniel J. Christensen¹, Charles Nicholson², Jeffrey J. Iliff¹, Takahiro Takano¹, Rashid Deane¹, and Maiken Nedergaard^{1,†}

¹Division of Glial Disease and Therapeutics, Center for Translational Neuromedicine, Department of Neurosurgery, University of Rochester Medical Center, Rochester, NY 14642, USA

²Department of Neuroscience and Physiology, Langone Medical Center, New York University, New York, NY 10016, USA

Abstract

The conservation of sleep across all animal species suggests that sleep serves a vital function. We here report that sleep has a critical function in ensuring metabolic homeostasis. Using real-time assessments of tetramethylammonium diffusion and two-photon imaging in live mice, we show that natural sleep or anesthesia are associated with a 60% increase in the interstitial space, resulting in a striking increase in convective exchange of cerebrospinal fluid with interstitial fluid. In turn, convective fluxes of interstitial fluid increased the rate of β -amyloid clearance during sleep. Thus, the restorative function of sleep may be a consequence of the enhanced removal of potentially neurotoxic waste products that accumulate in the awake central nervous system.

Despite decades of effort, one of the greatest mysteries in biology is why sleep is restorative and, conversely, why lack of sleep impairs brain function (1, 2). Sleep deprivation reduces learning, impairs performance in cognitive tests, prolongs reaction time, and is a common cause of seizures (3, 4). In the most extreme case, continuous sleep deprivation kills rodents and flies within a period of days to weeks (5, 6). In humans, fatal familial or sporadic insomnia is a progressively worsening state of sleeplessness that leads to dementia and death within months or years (7).

Proteins linked to neurodegenerative diseases, including β -amyloid (A β) (8), α -synuclein (9), and tau (10), are present in the interstitial space surrounding cells of the brain. In peripheral tissue, lymph vessels return excess interstitial proteins to the general circulation for degradation in the liver (11). Yet despite its high metabolic rate and the fragility of neurons to toxic waste products, the brain lacks a conventional lymphatic system. Instead, cerebrospinal fluid (CSF) recirculates through the brain, interchanging with interstitial fluid (ISF) and removing interstitial proteins, including A β (12, 13). The convective exchange of CSF and ISF is organized around the cerebral vasculature, with CSF influx around arteries, whereas ISF exits along veins. These pathways were named the glymphatic system on the basis of their dependence on astrocytic aquaporin-4 (AQP4) water channels and the adoption of functions homologous to peripheral lymphatic removal of interstitial metabolic

Copyright 2013 by the American Association for the Advancement of Science; all rights reserved.

[†]Corresponding author. nedergaard@urmc.rochester.edu.

*These authors contributed equally to this work.

Supplementary Materials

www.sciencemag.org/content/342/6156/373/suppl/DC1

Materials and Methods

Figs. S1 to S5

References

byproducts (14). Deletion of AQP4 channels reduces clearance of exogenous A β by 65%, suggesting that convective movement of ISF is a substantial contributor to the removal of interstitial waste products and other products of cellular activity (12). The interstitial concentration of A β is higher in awake than in sleeping rodents and humans, possibly indicating that wakefulness is associated with increased A β production (15, 16). We tested the alternative hypothesis that A β clearance is increased during sleep and that the sleep-wake cycle regulates glymphatic clearance.

We used in vivo two-photon imaging to compare CSF influx into the cortex of awake, anesthetized, and sleeping mice. The fluorescent tracers were infused into the subarachnoid CSF via a cannula implanted in the cisterna magna for real-time assessment of CSF tracer movement. Electroencephalography (EEG) and electromyography (EMG) were recorded in order to continuously monitor the state of brain activity (Fig. 1A and fig. S1). In initial experiments, the volume and rate of tracer infusion were adjusted so as to avoid changes in behavior state or EEG (fig. S1). Because mice sleep much of the day, a small molecular weight tracer, fluorescein isothiocyanate (FITC)-dextran (3 kD) in aCSF, was infused at midday (12 to 2 p.m.) via the cannula implanted in the cisterna magna. In sleeping mice, a robust influx of the fluorescent CSF tracer was noted along periarterial spaces, in the subpial regions, and in the brain parenchyma similar to previous findings in anesthetized mice (Fig. 1, B and C, and fig. S2) (12). EEG power spectrum analysis depicted a relatively high power of slow waves that is consistent with sleep (Fig. 1D). CSF tracer infusion (Texas red-dextran, 3 kD) was repeated in the same mouse after it was awakened through gentle handling of its tail. Unexpectedly, arousal sharply reduced tracer influx compared with that of the sleeping state. Periarterial and parenchymal tracer influx was reduced by ~95% in awake as compared with sleeping mice during the 30-min imaging session (Fig. 1, B and C, and fig. S2). EEG showed a reduction in the relative prevalence of slow (delta) waves concomitant with a significant increase in the power of fast activity, confirming that the animals were awake ($n = 6$ mice, $P < 0.05$, paired t test) (Fig. 1D). To investigate whether the state of brain activity indeed controlled CSF influx, we repeated the experiments in a new cohort of mice in which all experiments were performed when the animals were awake (8 to 10 p.m.). Because mice normally do not sleep at this time of day, we first evaluated CSF tracer influx in the awake state by means of intracisternal infusion of FITC-dextran. CSF tracer influx into the brain was largely absent and only slowly gained access to the superficial cortical layers (Fig. 1, E and F, and fig. S2). After 30 min imaging of CSF tracer in the awake state, the animals were anesthetized with intraperitoneal administration of ketamine/xylazine (KX). Texas red-dextran was administered 15 min later, when a stable increase in slow wave activity was noted (Fig. 1, E and F). Texas red-dextran rapidly flushed in along periarterial spaces and entered the brain parenchyma at a rate comparable with that of naturally sleeping mice (Fig. 1, B and E). Ketamine/xylazine anesthesia significantly increased influx of CSF tracer in all mice analyzed [$n = 6$ mice, $P < 0.05$, two-way analysis of variance (ANOVA) with Bonferroni test], which was concomitant with a significant increase in the power of slow wave activity ($n = 6$ mice, $P < 0.05$, paired t test) (Fig. 1, G and F). Thus, glymphatic CSF influx is sharply suppressed in conscious alert mice as compared with naturally sleeping or anesthetized littermates.

Influx of CSF is in part driven by arterial pulse waves that propel the movement of CSF inward along periarterial spaces (12). It is unlikely that diurnal fluctuations in arterial pulsation are responsible for the marked suppression of convective CSF fluxes during wakefulness because arterial blood pressure is higher during physical activity. An alternative possibility is that the awake brain state is linked to a reduction in the volume of the interstitial space because a constricted interstitial space would increase resistance to convective fluid movement and suppress CSF influx. To assess the volume and tortuosity of the interstitial space in awake versus sleeping mice, we used the real-time iontophoretic

tetramethyl-ammonium (TMA) method in head-fixed mice (Fig. 2A and fig. S3) (17, 18). TMA recordings in cortex of sleeping mice collected at midday (12 to 2 p.m.) confirmed that the interstitial space volume fraction (α) averaged $23.4 \pm 1.9\%$ ($n = 6$ mice) (19). However, the interstitial volume fraction was only $14.1 \pm 1.8\%$ in awake mice recorded at 8 to 10 p.m. ($n = 4$ mice, $P < 0.01$, t test) (Fig. 2B). Analysis of cortical ECoG recorded by the TMA reference electrode confirmed that the power of slow wave activity was higher in sleeping than in awake mice, which is concurrent with a lower power of high-frequency activity (Fig. 2C).

To further validate that the volume of the interstitial space differed in awake versus sleeping mice, we also obtained TMA recordings in awake mice in the late evening (8 to 10 p.m.) and repeated the recordings in the same mice after administration of ketamine/xylazine. This approach, which eliminated interanimal variability in electrode placement and TMA calibration, showed that anesthesia consistently increased the interstitial space volume fraction by $>60\%$, from $13.6 \pm 1.6\%$ for awake mice to $22.7 \pm 1.3\%$ in the same mice after they received ketamine/xylazine ($n = 10$ mice, $P < 0.01$, paired t test) (Fig. 2D). Analysis of ECoG activity extracted from the TMA reference electrode showed that ketamine/xylazine increased the power of slow wave activity in all animals analyzed (Fig. 2E). Thus, the cortical interstitial volume fraction is 13 to 15% in the awake state as compared to 22 to 24% in sleeping or anesthetized mice. Tortuosity of the interstitial space did not differ significantly according to changes in the state of brain activity; awake, sleeping, and anesthetized mice all exhibited a λ value in the range of 1.3 to 1.8, which is consistent with earlier reports ($n = 4$ to 10 mice, $P > 0.1$, t test) (Fig. 2, B and D) (19–21). Recordings obtained 300 μm below the cortical surface did not differ significantly from those obtained at 150 μm , suggesting that preparation of the cranial window was not associated with tissue injury ($n = 6$ mice, $P > 0.4$, t test) (Fig. 2D and fig. S3D). Other reports have shown that the interstitial volume is $\sim 19\%$ in anesthetized young mice but declines to $\sim 13\%$ in aged mice (22). Collectively, these observations support the notion that influx of CSF tracers is suppressed in awake mice as a result of contraction of the interstitial space: The smaller space during wakefulness increases tissue resistance to interstitial fluid flux and inward movement of CSF. This effect of arousal state on interstitial volume likely holds major implications for diffusion of neurotransmitters, such as glutamate (23).

Because previous analysis indicates that as much as 65% of exogenously delivered A β is cleared by the glymphatic system (12), we tested whether interstitial A β is cleared most efficiently during sleep. Radiolabeled ^{125}I -A β_{1-40} was injected intracortically in three groups of animals: freely behaving awake mice, naturally sleeping mice, and animals anesthetized with ketamine/xylazine (fig. S4). Brains were harvested 10 to 240 min later for analysis of ^{125}I -A β retention. A β was cleared twofold faster in the sleeping mice as compared with the awake mice ($n = 23$ to 29 mice, $P < 0.05$, ANOVA with Bonferroni test) (Fig. 3, A and B, $P < 0.05$). A β clearance did not differ between sleeping and anesthetized mice. Because A β is also removed from CNS via receptor-mediated transport across the blood-brain barrier (24), we also analyzed the clearance of an inert tracer, ^{14}C -inulin. ^{14}C -inulin was cleared more efficiently (greater than twofold) in sleeping and anesthetized mice as compared with awake mice (Fig. 3, C and D).

What drives the brain state-dependent changes of the interstitial space volume? The observation that anesthesia increases glymphatic influx and efflux (Figs. 1 and 3), suggests that it is not circadian rhythm but rather the sleep-wake state itself that determines the volume of the interstitial space and therefore the efficiency of glymphatic solute clearance. Arousal is driven by the concerted release of neuromodulators (25). In particular, locus coeruleus-derived noradrenergic signaling appears critical for driving cortical networks into the awake state of processing (26, 27). In peripheral tissues, such as kidney and heart,

noradrenaline regulates the activity of membrane transporters and channels that control cell volume (28). We hypothesized that adrenergic signaling in the awake state modifies cell volume and thus the size of the interstitial space. We first assessed whether suppression of adrenergic signaling in the awake conscious brain can enhance glymphatic tracer influx by pre-treating awake mice with a cocktail of adrenergic receptor antagonists or vehicle (aCSF) 15 min before infusion of fluorescent CSF tracers (27). The adrenergic receptor antagonists were administered through a cannula inserted into the cisterna magna, with an initial bolus followed by slow continuous drug infusion. Administration of adrenergic antagonists induced an increase in CSF tracer influx, resulting in rates of CSF tracer influx that were more comparable with influx observed during sleep or anesthesia than in the awake state (Fig. 4, A and B, and fig. S5). We asked whether increases in the level of norepinephrine (NE) resulting from stress during restraining at the microscope stage affected the observations. Microdialysis samples of the interstitial fluid showed that the NE concentration did not increase in trained mice during restraining but that NE, as expected, fell after administration of ketamine/xylazine (Fig. 4C).

We next evaluated whether adrenergic receptor inhibition increased interstitial volume in the same manner as sleep and anesthesia. We used the TMA method to quantify the effect of local adrenergic inhibition on the volume of the interstitial space. To restrict adrenergic inhibition to the cortex, receptor antagonists were applied directly to the exposed cortical surface rather than intracisternal delivery. TMA recordings showed that inhibition of adrenergic signaling in cortex increased the interstitial volume fraction from $14.3 \pm 5.2\%$ to $22.6 \pm 1.2\%$ ($n = 4$ to 8 mice, $P < 0.01$, t test). Interstitial volume was significantly greater than in awake littermates exposed to vehicle (aCSF) ($P < 0.01$) but comparable with the interstitial volume in sleeping or anesthetized mice ($P = 0.77$ and $P = 0.95$, respectively, t test) (Fig. 4D). Cortical ECoG displayed an increase in the power of slow waves when exposed to adrenergic receptor antagonists ($n = 7$ mice, $P < 0.01$, one-way ANOVA with Bonferroni test). In accordance with earlier findings (27), analysis of the power spectrum showed that inhibition of adrenergic signaling transformed the cortical ECoG of awake mice into a more sleep-like, albeit less regular, profile (Fig. 4E). These analyses suggest that adrenergic signaling plays an important role in modulating not only cortical neuronal activity but also the volume of the interstitial space. NE triggers rapid changes in neural activity (27, 28), which in turn can modulate the volume of the interstitial space volume (29). Nevertheless, additional analysis is clearly required to determine which cell types contribute to expansion of the interstitial space volume during sleep, anesthesia, or blockade of NE receptors (Figs. 2, B to D, and 4D).

Because of the high sensitivity of neural cells to their environment, it is essential that waste products of neural metabolism are quickly and efficiently removed from the brain interstitial space. Several degradation products of cellular activity, such as A β oligomers and amyloid depositions, have adverse effects on synaptic transmission (30) and cytosolic Ca²⁺ concentrations (31) and can trigger irreversible neuronal injury (32). The existence of a homeostatic drive for sleep—including accumulation of a “need to sleep” substance during wakefulness that dissipates during sleep—has been proposed (33). Because biological activity is inevitably linked to the production of metabolic degradation products, it is possible that sleep subserves the important function of clearing multiple potentially toxic CNS waste products. Our analysis indicates that the cortical interstitial space increases by more than 60% during sleep, resulting in efficient convective clearance of A β and other compounds (Figs. 2 and 3). The purpose of sleep has been the subject of numerous theories since the time of the ancient Greek philosophers (34). An extension of the findings reported here is that the restorative function of sleep may be due to the switching of the brain into a functional state that facilitates the clearance of degradation products of neural activity that accumulate during wakefulness.

Supplementary Material

Refer to Web version on PubMed Central for supplementary material.

Acknowledgments

This study was supported by NIH/National Institute of Neurological Disorders and Stroke (NS078167 and NS078304 to M.N. and NS028642 to C.N.). We thank S. Veasey for comments on the manuscript.

References and Notes

1. Saper CB, Fuller PM, Pedersen NP, Lu J, Scammell TE. *Neuron*. 2010; 68:1023–1042. [PubMed: 21172606]
2. Hobson JA. *Nature*. 2005; 437:1254–1256. [PubMed: 16251949]
3. Malow BA. *Epilepsy Curr*. 2004; 4:193–195. [PubMed: 16059497]
4. Stickgold R. *Nature*. 2006; 444:559–560. [PubMed: 17086196]
5. Rechtschaffen A, Gilliland MA, Bergmann BM, Winter JB. *Science*. 1983; 221:182–184. [PubMed: 6857280]
6. Shaw PJ, Tononi G, Greenspan RJ, Robinson DF. *Nature*. 2002; 417:287–291. [PubMed: 12015603]
7. Montagna P, Gambetti P, Cortelli P, Lugaresi E. *Lancet Neurol*. 2003; 2:167–176. [PubMed: 12849238]
8. Cirrito JR, et al. *Neuron*. 2005; 48:913–922. [PubMed: 16364896]
9. Larson ME, et al. *J Neurosci*. 2012; 32:10253–10266. [PubMed: 22836259]
10. Yamada K, et al. *J Neurosci*. 2011; 31:13110–13117. [PubMed: 21917794]
11. Aukland K, Reed RK. *Physiol Rev*. 1993; 73:1–78. [PubMed: 8419962]
12. Iliff JJ, et al. *Sci Transl Med*. 2012; 4:147ra111.
13. Iliff JJ, et al. *J Clin Invest*. 2013; 123:1299–1309. [PubMed: 23434588]
14. Nedergaard M. *Science*. 2013; 340:1529–1530. [PubMed: 23812703]
15. Bateman RJ, et al. *Nat Med*. 2006; 12:856–861. [PubMed: 16799555]
16. Kang JE, et al. *Science*. 2009; 326:1005–1007. [PubMed: 19779148]
17. Nicholson C, Phillips JM. *J Physiol*. 1981; 321:225–257. [PubMed: 7338810]
18. Nicholson C. *J Neurosci Methods*. 1993; 48:199–213. [PubMed: 8412303]
19. Yao X, Hrabetová S, Nicholson C, Manley GT. *J Neurosci*. 2008; 28:5460–5464. [PubMed: 18495879]
20. Nicholson C, Syková E. *Trends Neurosci*. 1998; 21:207–215. [PubMed: 9610885]
21. Syková E, Nicholson C. *Physiol Rev*. 2008; 88:1277–1340. [PubMed: 18923183]
22. Syková E, et al. *Proc Natl Acad Sci USA*. 2005; 102:479–484. [PubMed: 15630088]
23. Kinney JP, et al. *J Comp Neurol*. 2013; 521:448–464. [PubMed: 22740128]
24. Deane R, et al. *J Clin Invest*. 2008; 118:4002–4013. [PubMed: 19033669]
25. Steriade M, McCormick DA, Sejnowski TJ. *Science*. 1993; 262:679–685. [PubMed: 8235588]
26. Carter ME, et al. *Nat Neurosci*. 2010; 13:1526–1533. [PubMed: 21037585]
27. Constantinople CM, Bruno RM. *Neuron*. 2011; 69:1061–1068. [PubMed: 21435553]
28. O'Donnell J, Zeppenfeld D, McConnell E, Pena S, Nedergaard M. *Neurochem Res*. 2012; 37:2496–2512. [PubMed: 22717696]
29. McBain CJ, Traynelis SF, Dingledine R. *Science*. 1990; 249:674–677. [PubMed: 2382142]
30. Parameshwaran K, Dhanasekaran M, Suppiramaniam V. *Exp Neurol*. 2008; 210:7–13. [PubMed: 18053990]
31. Kuchibhotla KV, et al. *Neuron*. 2008; 59:214–225. [PubMed: 18667150]
32. Mattson MP. *Ann N Y Acad Sci*. 1994; 747:50–76. [PubMed: 7847692]
33. Borbely, A.; Tobler, I. *Brain Mechanisms of Sleep*. McGinty, DJ., editor. Raven; New York: 1985. p. 35-44.

34. Barbera J. *Sleep Med.* 2008; 9:906–910. [PubMed: 19014776]

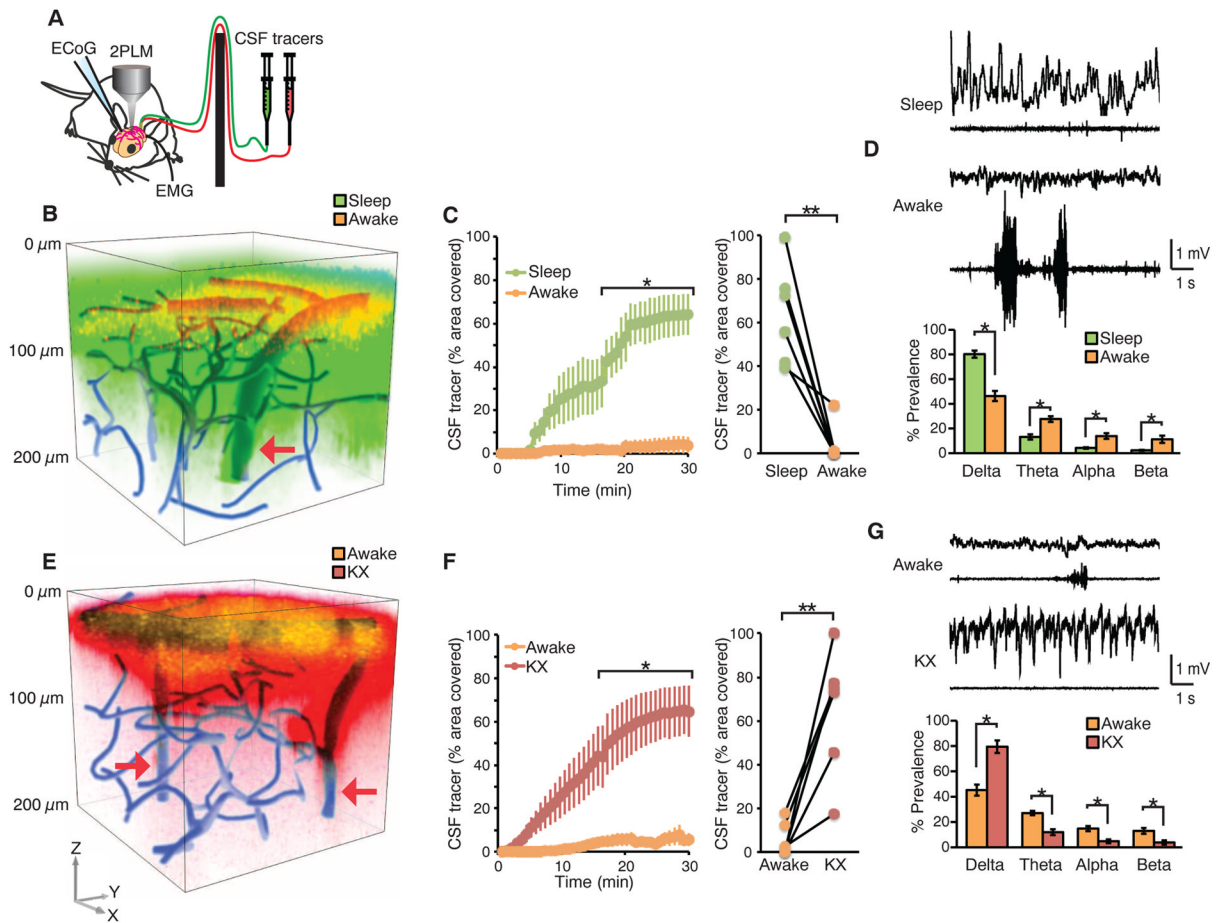


Fig. 1. Wakefulness suppresses influx of CSF tracers

(A) Diagram of experimental setup used for two-photon imaging of CSF tracer movement in real time. To avoid disturbing the state of brain activity, a cannula with dual ports was implanted in the cisterna magna for injection of CSF tracers. ECoG and EMG were recorded to monitor the state of brain activity. (B) Three-dimensional (3D) vectorized reconstruction of the distribution of CSF tracers injected in a sleeping mouse and then again after the mouse was awakened. The vasculature was visualized by means of cascade blue-dextran administered via the femoral vein. FITC-dextran (green) was first injected in the cisterna magna in a sleeping mouse and visualized by collecting repeated stacks of z-steps. Thirty min later, the mouse was awakened by gently moving its tail, and Texas red-dextran (red) was administered 15 min later. The experiments were performed mostly asleep (12 to 2 p.m.). The arrow points to penetrating arteries. (C) Comparison of time-dependent CSF influx in sleep versus awake. Tracer influx was quantified 100 μm below the cortical surface; $n = 6$ mice; $*P < 0.05$, two-way ANOVA with Bonferroni test. (Right) The tracer intensity within the two arousal states at the 30-min time point was compared. $**P < 0.01$, t test. (D) ECoG and EMG recordings acquired during sleep and after the mouse was awakened. Power spectrum analysis of all the animals analyzed in the two arousal states ($n = 6$ mice; $*P < 0.05$, t test). (E) 3D reconstruction of CSF tracer influx into the mouse cortex. FITC-dextran was first injected in the awake stage, and cortical influx was visualized by means of two-photon excitation for 30 min. The mouse was then anesthetized with ketamine/xylazine (intraperitoneally), and Texas red-dextran was injected intra-cisternally 15 min later. The vasculature was visualized by means of cascade blue-dextran. Arrows point to penetrating arteries. (F) Comparison of time-dependent CSF influx in awake versus

ketamine/xylazine anesthesia; $n = 6$ mice; $*P < 0.05$, two-way ANOVA with Bonferroni test. (Right) The tracer intensity during the two arousal states at the 30-min time point was compared. $**P < 0.01$, t test. (G) ECoG and EMG recordings in the awake mouse and after administration of ketamine/xylazine. Power spectrum analysis of all the animals analyzed in the two arousal states; $n = 6$ mice; $*P < 0.05$, t test.

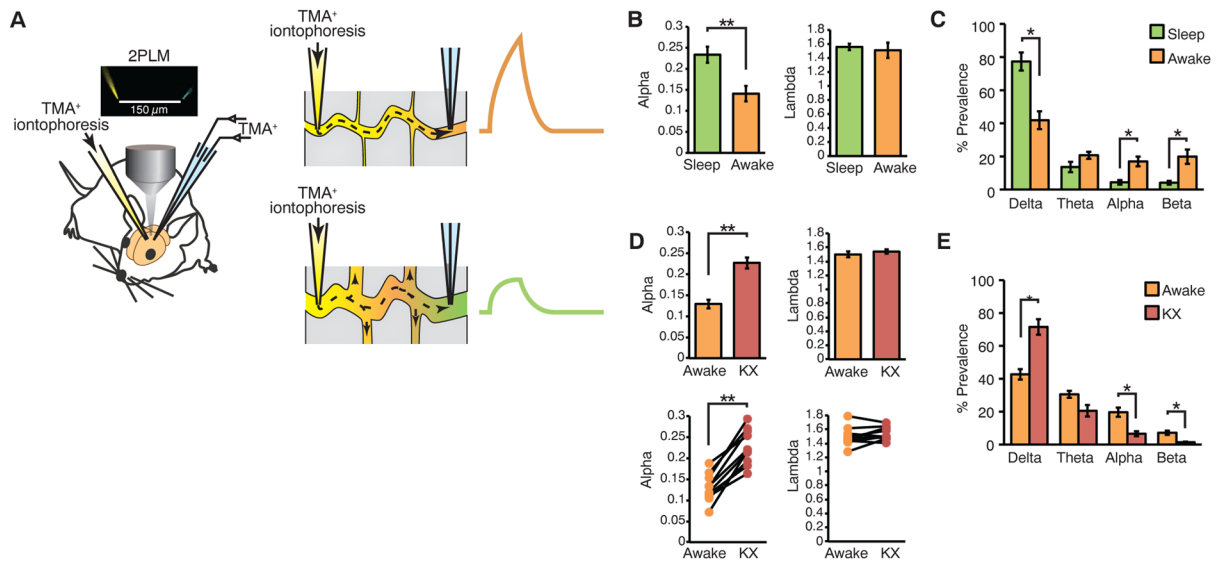


Fig. 2. Real-time TMA⁺ iontophoretic quantification of the volume of the extracellular space in cortex

(A) TMA⁺ was delivered with an ion-tophoresis microelectrode during continuous recordings by a TMA⁺-sensitive microelectrode located a distance of ~150 μm away. The electrodes were filled with Alexa488 and Alexa568, respectively, so that their distance could be determined with two-photon excitation (insert over objective). A smaller extracellular space results in reduced TMA⁺ dilution, reflected by higher levels of detected TMA⁺. (B) The extracellular space is consistently smaller in awake than in sleeping mice, whereas the tortuosity remained unchanged (λ); $n = 4$ to 6 mice; $**P < 0.01$, t test. (C) Power spectrum analysis of ECoG recordings; $n = 6$ mice; $*P < 0.05$, t test. (D) The extracellular space was consistently smaller in the awake state than after administration of ketamine/xylozazine in paired recordings within the same mouse, whereas tortuosity did not change after anesthesia; $n = 10$ mice; $**P < 0.01$, t test. (Bottom) TMA measurements obtained during the two arousal states compared for each animal. (E) Power spectrum analysis of ECoG; $n = 6$ mice; $*P < 0.05$, t test.

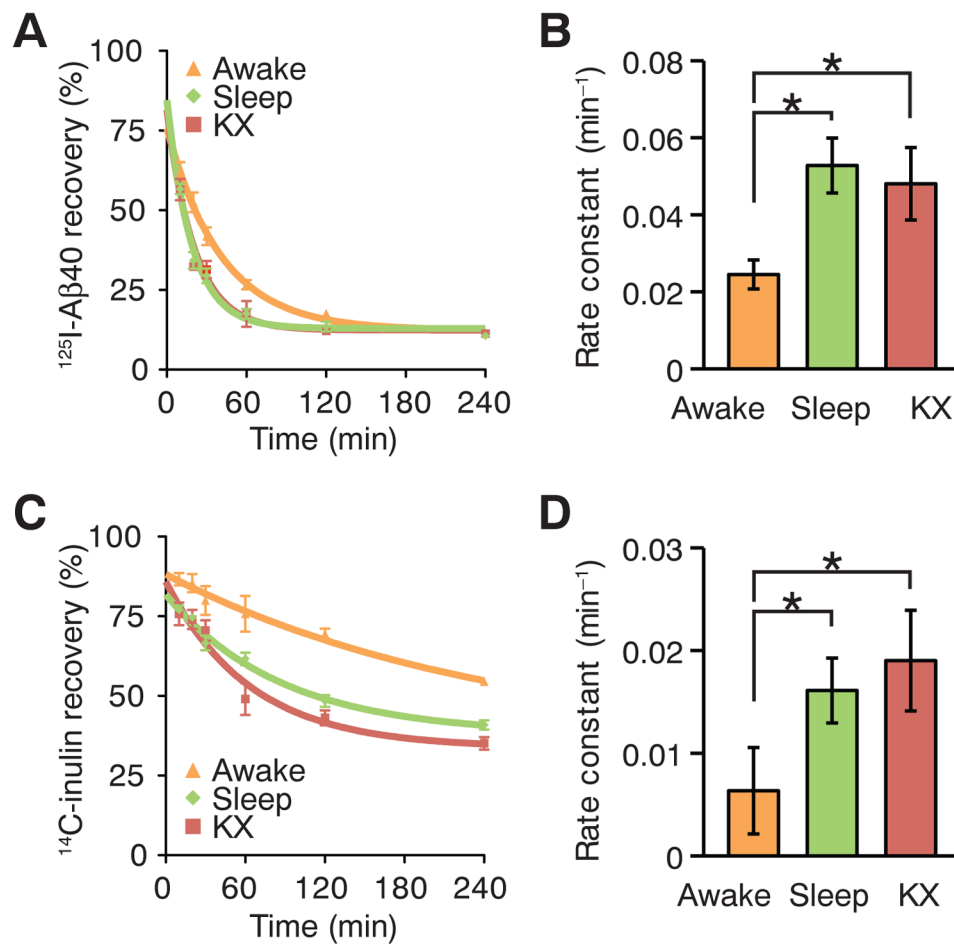


Fig. 3. Sleep improves clearance of A β

(A). Time-disappearance curves of $^{125}\text{I-A}\beta_{1-40}$ after its injection into the frontal cortex in awake (orange triangles), sleeping (green diamonds), and anesthetized (red squares, ketamine/xylazine) mice. (B) Rate constants derived from the clearance curves. (C) Time-disappearance curves of $^{14}\text{C-inulin}$ after its injection into the frontal cortex of awake (orange triangles), sleeping (green diamonds), and anesthetized (red squares, ketamine/xylazine) mice. (D) Rate constants derived from the clearance curves. A total of 77 mice were included in the analysis: 25 awake, 29 asleep, and 23 anesthetized, with 3 to 6 mice per time point. * $P < 0.05$ compared with awake, ANOVA with Bonferroni test.

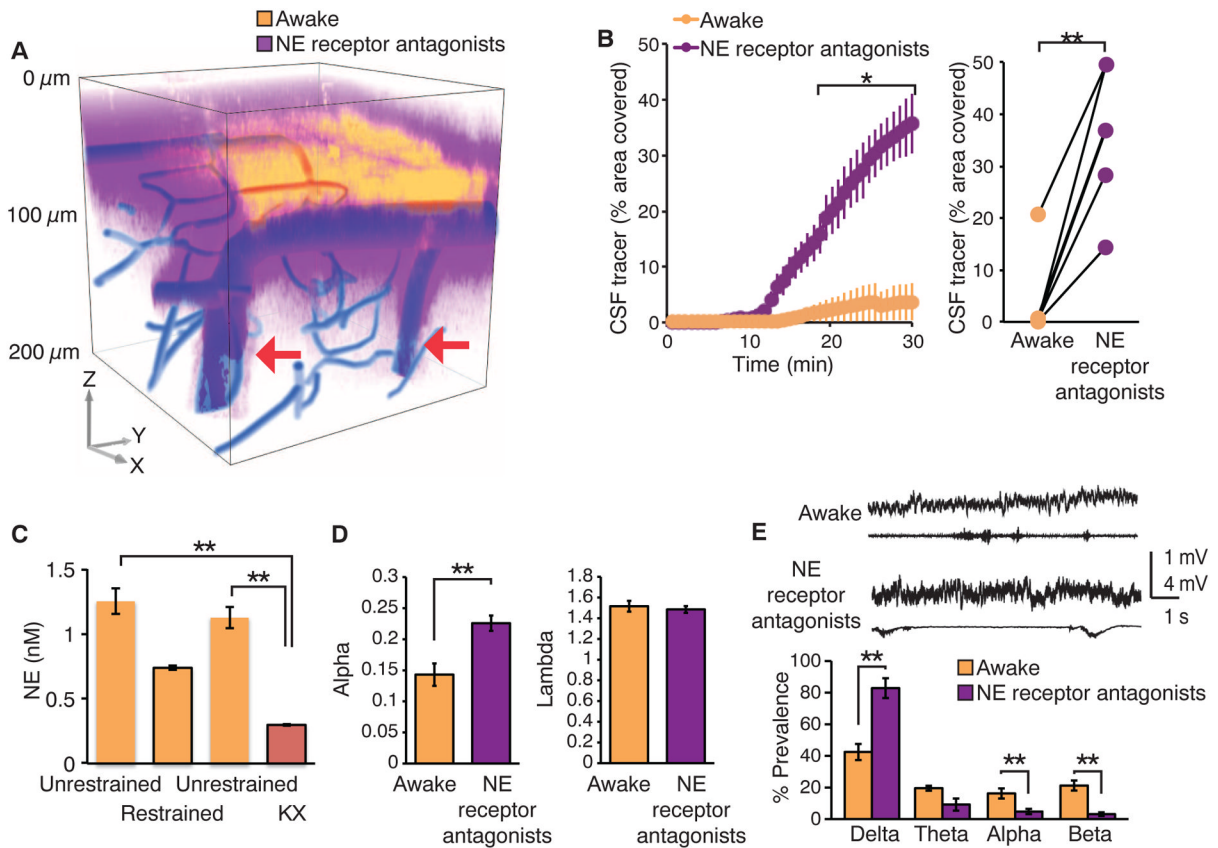


Fig. 4. Adrenergic inhibition increases CSF influx in awake mice

(A) CSF tracer influx before and after intracisternal administration of a cocktail of adrenergic receptor antagonists. FITC-dextran (yellow, 3 kD) was first injected in the cisterna magna in the awake mouse, and cortical tracer influx was visualized by means of two-photon excitation for 30 min. The adrenergic receptor antagonists (prazosin, atipamezole, and propranolol, each 2 mM) were then slowly infused via the cisterna magna cannula for 15 min followed by injection of Texas red-dextran (purple, 3 kD). The 3D reconstruction depicts CSF influx 15 min after the tracers were injected in cisterna magna. The vasculature was visualized by means of cascade blue-dextran. Arrows point to penetrating arteries. (B) Comparison of tracer influx as a function of time before and after administration of adrenergic receptor antagonists. Tracer influx was quantified in the optical section located 100 μm below the cortical surface; $n = 6$ mice; $*P < 0.05$, two-way ANOVA with Bonferroni test. (Right) The tracer intensity during the two arousal states at the 30-min time point was compared. $**P < 0.01$, t test. (C) Comparison of the interstitial concentration of NE in cortex during head-restraining versus unrestrained (before and after), as well as after ketamine/xylazine anesthesia. Microdialysis samples were collected for 1 hour each and analyzed by using high-performance liquid chromatography. $**P < 0.01$, one-way ANOVA with Bonferroni test. (D) TMA⁺ iontophoretic quantification of the volume of the extracellular space before and after adrenergic inhibition; $n = 4$ to 8 mice; $**P < 0.01$, t test. (E) Power spectrum analysis, $n = 7$ mice; $**P < 0.01$, one-way ANOVA with Bonferroni test.